System to Guide Transcatheter Aortic Valve Implantations Based on Interventional C-Arm CT Imaging

Matthias John[1], Rui Liao[2], Yefeng Zheng[2], Alois Nöttling[1], Jan Boese[1], Uwe Kirschstein[1], Jörg Kempfert[3], Thomas Walther[4]

[1] Siemens AG, Healthcare Sector, Forchheim, Germany
[2] Siemens Corporate Research, Princeton, USA
[3] Department of Cardiac Surgery, Heart Center, University of Leipzig, Germany
[4] Department of Cardiac Surgery, Kerckoff Heart Center, Bad Nauheim, Germany
matthias.mj.john@siemens.com

Abstract. Transcatheter aortic valve implantation is an emerging technique to be applied in patients with aortic valve defects. Angiographic and fluoroscopic X-ray imaging with a C-arm system is crucial in these minimal invasive procedures. We describe a prototypical system, that allows to perform 3D C-arm CT imaging during transcatheter aortic valve implantations. It supports the physician in measuring critical anatomical parameters, finding an optimum C-arm angulation, and guiding the positioning and deployment of the prosthesis by 3D overlay upon the fluoroscopic images. To yield high acceptance by the physicians in the operating room, our approach is fast, fully integrated into an angiographic C-arm system, and designed to minimize the necessary user interaction. We evaluate the accuracy of our system in 20 clinical cases.

1 Introduction

Aortic valve disease is the most common valvular problem in old age. A minimal invasive transcatheter aortic valve implantation (TAVI) can be performed in high risk patients with a severe aortic stenosis. It has the potential to be applied to regular risk patients instead of an open heart surgery including sternotomy, extracorporeal circulation and cardioplegic cardiac arrest. A bio-prosthesis is positioned and deployed via a catheter in the aortic root of the patient. During transapical TAVI an antegrade access is used where the catheter and the prosthesis are inserted via small incisions in the chest and the apex of the left ventricle. During transfemoral TAVI the catheter is inserted retrogradely via the femoral artery and the aortic arch. Both approaches require X-ray angiographic and fluoroscopic imaging to guide the procedure (see Figure 1). Therefore these procedures are usually performed in operating rooms equipped with a fixed angiographic C-arm system (“Hybrid OR”). To make the anatomy of the aortic root visible under X-ray, contrast agent must be injected. Due to renal insufficiencies in these patients the amount of contrast agent must be minimized.

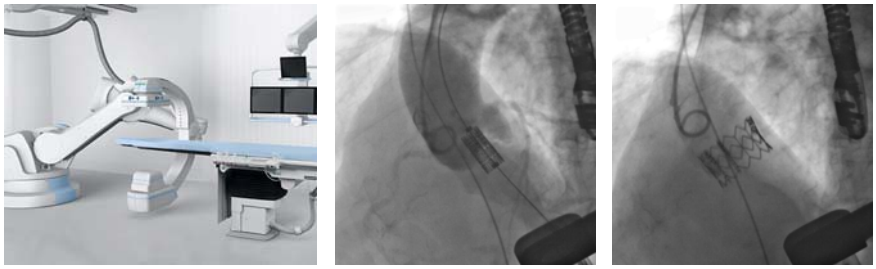

Fig. 1. Transapical aortic valve implantation under X-ray guidance. **Left:** Angiographic C-arm system able to acquire interventional 3D images in an operating room. **Middle:** Contrast injection via pigtail catheter immediately prior to valve deployment. **Right:** Implanted valve.

Prior to implantation it is important to angulate the C-arm with respect to the aortic root anatomy of the patient. Rotational symmetric prostheses require an angulation perpendicular to the aortic root to be placed correctly. Prostheses that model the leaflet anatomy require an angulation that allows to outline the commissures (connection of the valvular leaflets). Usually, an appropriate angulation is achieved with iterated C-arm angulations, each followed by an angiogram of approximately 15 ml contrast to double-check the aortic root position. Further angiograms are needed later on for correct prosthesis positioning and for functional control after implantation.

Our goal is to provide image guidance based on interventional C-arm CT images to add detailed 3D information to the procedure. The system needs to be set up in the complex environment of an operating room and used by a physician during a TAVI. Therefore, it is crucial for the acceptance of such a system to be fast, to minimize the user interaction and to allow table-side control.

Previous work about the support of transcatheter aortic valve implantations containes the modeling for procedure planning [1,2], guidance by tracking the prosthesis in fluoroscopic images [3], and a robotic system using MRI imaging [4].

2 Method

In this section we describe the design of our system. We follow the steps the system performs during transcatheter aortic valve implantation and discuss the user interactions. All described components were prototypically integrated into an angiographic C-arm system (Artis zee/zeego with syngo workplace, Siemens, Erlangen, Germany).

Right before the implantation the physician starts to obtain an interventional 3D image of the aortic root by acquiring a rotational 2D image sequence of 200° over 5 seconds on the C-arm system. Via a pigtail catheter 25 ml contrast agent (diluted to 75 ml) is injected over 5 seconds (with a 1-second X-ray delay) into the aortic root. To minimize motion artifacts we stop patient breathing and apply rapid ventricular pacing to a heart rate that yields no heart pumping and minimizes blood flow. This allows to use a relatively small amount of contrast agent - compared to approximately 80 ml for a conventional CT and approximately 15 ml for a single 2D angiogram [5].

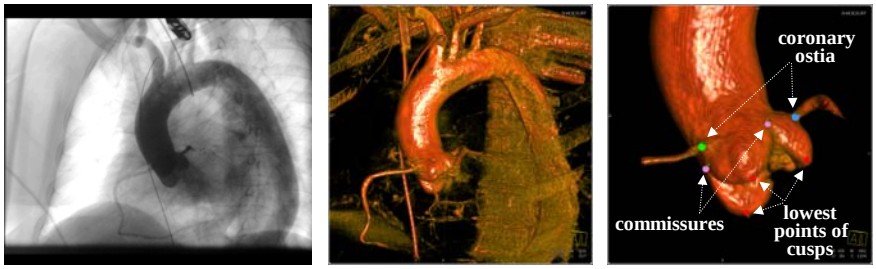

Fig. 2. Left: Image from a rotational acquisition scene acquired under rapid ventricular pacing and contrast injection into aortic root. **Middle:** C-arm CT image reconstructed from this scene. **Right:** Segmented aortic root with landmarks.

After the rotational run is finished on the C-arm system, all of the following steps 1–7 are started and performed fully automatically.

1. Reconstructing 3D data from acquired rotational image sequence.

The rotational run is reconstructed based on a software available with the angiographic C-arm system [6] (see Figure 2), which takes about 12 seconds.

2. Detecting aortic root shape and landmarks from 3D volume.

Following [5] we detect the aortic root shape and eight landmarks (see Figure 2, right): the lowest point of each aortic root cusp (to support finding a C-arm angulation perpendicular to the aortic root), the coronary artery ostia (which have to stay open after prostheses implantation), the commissure points where the cusps meet (to help orienting anatomically designed valve prostheses) and finally the centerline.

We use a fast dedicated machine learning based algorithm [7]: First, position, orientation, and scale of the aortic root are estimated by the efficient Marginal Space Learning (MSL) algorithm. Then the mean aortic root shape (calculated from a training set) is aligned with the estimated pose, followed by boundary refinement using a learning-based 3D boundary detector. In addition, the eight landmarks are detected using a discriminative learning based landmark detector. The authors report the following mean detection errors based on a four-fold cross validation on a dataset with 192 volumes: 1.1 mm for aortic root mesh, 2.4 mm for lowest cusp points, 3.5 mm for the aortic commissure points, and 2.7 mm for the coronary ostia.

3. Deriving additional structures from detected landmarks.

We derive a circle parallel to the plane spanned by the three lowest points of the cusps (see red circle in Figure 3). Visually, this perpendicularity circle degenerates to a straight line if and only if the three lowest cusp points are aligned (see Figure 4), which corresponds to an optimal perpendicular angulation for valve implantation.

To estimate how critical the position of the coronary ostia is to stay open after implantation, the physician wants to measure their distance to the plane through the three lowest points of the cusps. We create a ruler orthogonal to that plane (see red ruler in Figure 3). We decided to show a ruler instead of numbers, because this makes the measurement process transparent to the physician and allows for user compensation of the measurement in case of misdetected landmarks.

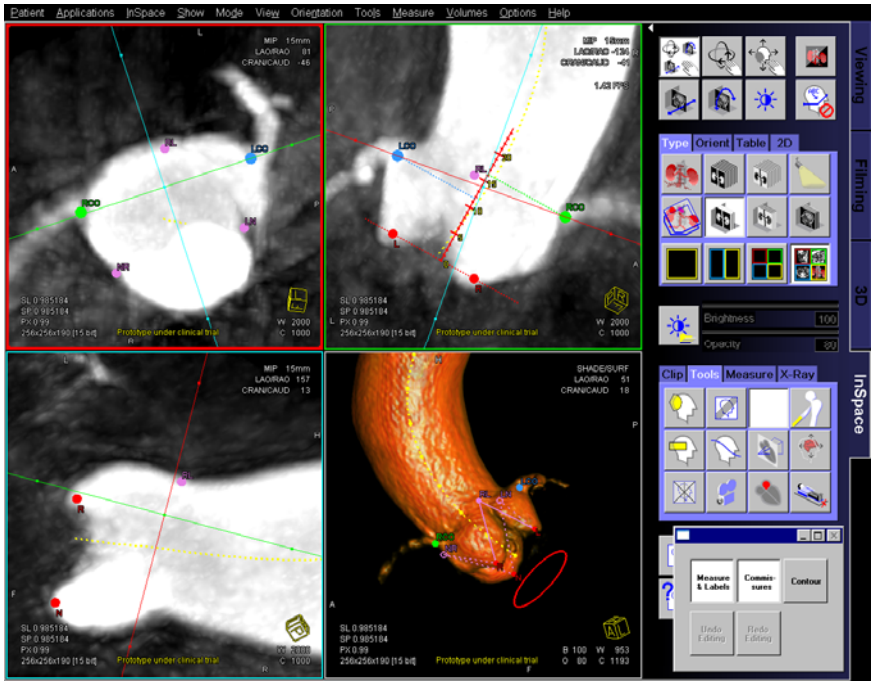

Fig. 3. System appearance after automatically performing steps 1-7. Detected landmarks (coronary ostia in blue and green, commissure points in purple, lowest points of cusps in red, centerline in yellow) and derived structures (perpendicularity circle and ruler in red) are shown in 3D volume rendering and three orthogonal intersection planes with 15 mm slice thickness. The panel in the lower right shows the user interface we added to the existing system.

4. Extract interior of detected aortic shape out of 3D volume for volume rendering.

The interior of the detected aortic root is extracted from the volume and visualized with volume rendering. We believe that with volume rendering it is easier for a user to justify the correctness of the detection step compared to a mesh visualization, because volume rendering still works on the original intensities of the image voxels.

A 100% correct aortic root detection can not be guaranteed for all patients. Therefore, we decided to dilate the extracted volumetric shape by 2 mm (determined heuristically) so that the user can visually detect accidentally removed structures. Also visualization of coronary arteries is important, but automatic segmentation is difficult. To make them visible without segmenting them explicitly we add a ball shape of 15 mm (determined heuristically) around each detected coronary ostium. This ensures that coronary artery segments are volume rendered even in cases of slight misdetections.

5. Computing optimized volume rendering transfer function parameters.

We want to avoid letting the user find manually the appropriate volume rendering parameters c_{opt} for transfer function center and w_{opt} for transfer function width. Therefore, they are calculated automatically based on the voxel intensities:

$$c_{opt} = f_{c,in}\, m_{in} + f_{c,out}\, m_{out} + f_{c,offset}$$
$$w_{opt} = f_{w,in}\, m_{in} + f_{w,out}\, m_{out} + f_{w,offset} \quad \textbf{(1)}$$

Here, m_{out} (m_{in}) is a volume specific value and is determined by the mean intensities of all voxels outside (inside) the boundary of the segmented aortic root with a fixed distance to it. The underlying set of voxels is computed using the morphologic operators dilation and erosion with a certain number of iterations. The six parameters $f_{c,in}$, $f_{c,out}$, $f_{w,offset}$, $f_{w,in}$, $f_{w,out}$, $f_{w,offset}$ in Equation 1 are fixed values that are obtained by a trained sample set of segmented volumes: For each of these training volumes we manually adjusted optimal window width and window center values. Together with the calculation of the corresponding values m_{in} and m_{out} we get an over-determined system of linear equations with six unknown parameters, which is then solved by a least-squares fit method.

6. Computing good volume position and orientations of intersection planes.

To give the user a good initial view, the volume is centered and zoomed based on the position of the two detected coronary ostia.

To allow the user an easy verification of the detected coronary ostia, we show two orthogonal volume intersection planes both containing the two ostia (see Figure 3). One of the planes is chosen to be orthogonal to the plane spanned by the three lowest points of the cusps. This plane contains the ruler discussed in step 3 and therefore allows the user to directly measure distances without any user interactions.

7. Visualizing 3D volume and intersection planes in a 2×2 screen.

According to the computations in the previous steps, the segmented aortic root volume is shown in a 3D volume rendering screen. Three orthogonal intersection planes show the unsegmented volume. All four screens contain the detected landmarks (see Figure 3). The perpendicularity circle is displayed in the 3D volume window and the ruler in one of the intersection planes. To allow for verification of the landmark detection (also in cases the detection went slightly wrong), we show the intersection planes as 15 mm thick maximum intensity projections (MIP).

After the results are presented, the physician is able to adjust landmarks and visualization if necessary. All described interactions can be done immediately at the operating table using a joystick equipped with the angiographic C-arm system.

8. Editing landmarks with automatic adaption of derived structures.

By drag and drop the user can edit the detected landmarks in the orthogonal intersection planes and in the volume rendering screen. Undo and redo functionality ensure that editing mistakes can be handled easily. Structures derived from the landmarks (like ruler, centerline and perpendicularity circle) are adapted in real-time.

9. Toggling on/off landmarks and structures.

Because displaying too many structures simultaneously can confuse the user, some of them can be toggled on and off (see user interface in Figure 3). The system can be configured in such a way, that the preferred set of structures is initially shown.

If landmark positions and visualization are satisfactory, the physician can perform the following steps:

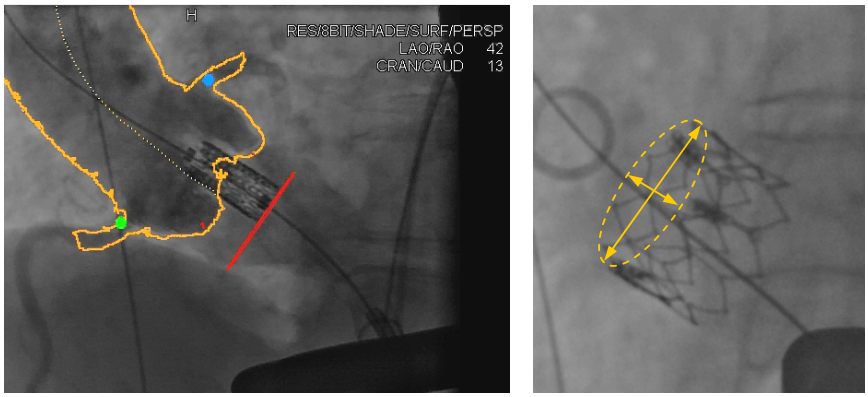

Fig. 4. Left: Overlay with perfect matching (measured misalignment is 0 mm). **Right:** Measurement of potential tilting of the prosthesis for evaluation (for better illustration we show an image from an angulation not used for valve deployment).

10. Rotating 3D volume to an appropriate C-arm angulation.

Every rotation of the volume rendering view corresponds to a C-arm angulation (up to in-plane rotation). Therefore, using the displayed perpendicularity circle or the commissure points, the physician can virtually choose a view that corresponds to an appropriate C-arm angulation. The system then allows to automatically rotate the C-arm to that angulation.

11. Switching to contour view.

When overlaying the 3D volume onto a live fluoroscopic scene, we offer a contour view of the aortic root which shows only the essential information needed for prosthesis positioning and deployment. Therefore, much less fluoroscopic image space is covered compared to volume rendering which yields better fluoroscopic image quality in the overlay for a safer implantation (see Figure 4, left).

The contours are computed by an efficient edge detection: First, a volume rendered aortic root image is segmented by simple image intensity thresholding. Second, gradients of the segmented pixels are calculated. The maximum gradient value is also assigned to border pixels (pixels with at least one neighboring background pixel). Third, edge pixels are detected by a hysteresis thresholding (similar to Canny edge detector) on the gradient values. Finally, connected components with a small number of detected edge pixels are removed.

12. Starting overlay of visualized 3D structures onto fluoroscopic images.

The live overlay of the rendered 3D visualization onto fluoroscopic images is based on a software available with the angiographic C-arm system. The 3D volume is inherently registered to the fluoroscopic images because both images are acquired on the same system. The overlay dynamically adapts to C-arm rotations and table movements. It does not compensate for patient and heart motions, but can be corrected manually in these cases. This mode can be used to adjust or fine-tune the C-arm angulation needed for implantation (see Figure 4, left).

3 Evaluation

We evaluated the accuracy of our system in patients who received an Edwards Sapien valve prosthesis (Edwards Lifesiences, Irvine, USA). These valves are deployed under rapid ventricular pacing. Retrospectively we analyzed the first 20 cases that were supported by our system and where the overlay image scene was documented.

First, we were interested how well the system can help to position the valve in the aortic root anatomy with a correct tilting. Assuming that a C-arm angulation adjusted with our system influences the final valve tilting, it would be interesting to evaluate the valve position in the patient anatomy. Unfortunately this would require the effort of a post-op 3D image scan including additional contrast agent and X-ray dose. Instead we determined for each patient the tilting angle of the implanted prosthesis in the 2D fluoroscopic image under the chosen angulation. Thereby we assume, that ideally an optimal angulation would result in a valve image not showing any tilting. With this assumption we ignore other factors like the complex interaction of operators, devices, and patient anatomy. We measured the ellipsoid diameters of the upper prosthesis ring in the image in pixels (see Figure 4, right) and derived the tilting by $90°-acos(diam_{min}/diam_{max})$. This value says how perpendicular the valve prosthesis was imaged right after implantation. For the 20 evaluated patients, we got a tilting of 5.7° ± 5.2° (mean ± standard deviation). Clinically, a tilting of < 5° can be stated as very good (obtained in 60% of the patients in our study), 5°-10° as good (30%), 10°-15° as acceptable (5%) and > 15° as inappropriate (5%). The values show that a procedure with 3D image support by our system yields overall good results. Reasons for suboptimal angulation estimation in some cases might be misdetections because of C-arm CT image artifacts, resulting from asymmetric position of the injection pigtail catheter in the aortic root and severe aortic regurgitation.

Second, we evaluated the accuracy of the overlay of the 3D image and the X-ray images. We assume that a misalignment corresponds to a shift parallel to the projection plane, which simplifies the evaluation but ignores rotations and zooming. For each patient we took an image from the recorded overlay scene that showed a contrast injection with rapid pacing right before deployment of the prosthesis (see Figure 4, left). Then we measured the shift error as the distance (in pixels) of a landmark point that could be identified in X-ray image and 3D overlay, e.g. lowest cusp point or coronary ostium. Furthermore we measured the shift along the aortic root centerline, which is the most important direction for guiding the implantation. Because of the projective geometry of the images, a measurement in pixels must be scaled using the known length of an object in approximately the same distance to the X-ray detector. For this we used the known length of the implanted prosthesis (in mm) divided by its measured height (in pixels). For the 20 evaluated patients we got a shift error of 3.1 mm ± 1.9 mm (mean ± standard deviation) and in centerline direction a shift error of 1.9 mm ± 1.5 mm. The reasons for pronounced deviation in a few patients could be the dislocation of the aortic root by sheath-manipulation and accidentally movements of the patients caused by the physicians. The measured accuracy is only valid under repeat rapid pacing, which recovers the heart position that we had during the 3D imaging and which minimizes heart motion.

4 Conclusion

The system design makes the use of interventional 3D imaging for transcatheter aortic valve implantations feasible and valuable. It is prototypically used in parallel to conventional fluoroscopy and angiography. The main benefits are the adjustment of an optimal C-arm angulation based on 3D information requiring only a low amount of contrast agent, the measurement of the critical coronary ostia distances and the additional anatomical orientation by the fluoroscopic overlay when implanting the valve.

The system is very fast: the post-processing of the 3D data (steps 2-7 in section 2) takes about 4 seconds. In the cases done up to now all described algorithm steps were running stably. In practice, landmark adjustments were only rarely done by the user. In this cases the table sided joystick was an appropriate tool which eliminates the need to operate a mouse in the unsterile environment of the control room.

Valuable extensions of our system would be an automated motion compensation of the 3D overlay on fluoroscopic images and the integration of pre-operative CT images. For evaluation purposes it would be interesting to compare our proposed system with the conventional approach to implant aortic valves.

References

1. Gessat, M.; Merk, D.R.; Falk, V.; Walther, T.; Jacobs, S.; Nöttling, A.; Burgert, O.: A planning system for transapical aortic valve implantation. Medical Imaging: Visualization, Image-Guided Procedures, and Modeling, vol. 7261, SPIE, 2009.
2. Ionasec, R.; Georgescu, B.; Gassner, E.; Vogt, S.; Kutter, O.; Scheuering, M.; Navab, N.; Comaniciu, D.: Dynamic model-driven quantification and visual evaluation of the aortic valve from 4D CT. Medical Image Computing and Computer Assisted Intervention (MICCAI), 2008.
3. Karar, M.E.; Chalopin, C.; Merk, D.R.; Jacobs, S.; Walther, T.; Falk, V.; Burgert, O.: Localization and tracking of aortic valve prosthesis in 2D fluoroscopic image sequences. Medical Imaging: Visualization, Image-Guided Procedures, and Modeling, vol. 7261, SPIE, 2009.
4. Li, M.; Mazilu, D.; Horvath, K.A.: Robotic System for Transapical Aortic Valve Replacement with MRI Guidance. Medical Image Computing and Computer Assisted Intervention (MICCAI), 2008.
5. Kempfert, J.; Falk, V.; Schuler, G.; Linke, A.; Merk, D.R.; Mohr, F.W.; Walther, T.: Dyna-CT during minimally invasive off-pump transapical aortic valve implantation. Ann Thorac Surg. 88(6):2041, 2009.
6. Zellerhoff, M.; Scholz, B.; Ruehrnschopf, E.-P.; Brunner, T.: Low contrast 3D reconstruction from C-arm data. Medical Imaging: Physics of Medical Imaging, vol. 5745, SPIE, 2005.
7. Zheng, Y.; John, M.; Liao, R.; Boese, J.; Kirschstein, U.; Georgescu, B.; Zhou, S.K.; Kempfert, J.; Walther, T.; Brockmann, G.; Comaniciu, D.: Automatic Aorta Segmentation and Valve Landmark Detection in C-Arm CT: Application to Aortic Valve Implantation. Medical Image Computing and Computer Assisted Intervention (MICCAI), 2010.